Chapter 19

ON THE ELECTRON-ELECTRON INTERACTIONS IN TWO DIMENSIONS

V. M. Pudalov
P. N. Lebedev Physics Institute, Moscow 119991, Russia

M. Gershenson and H. Kojima
Physics and Astronomy, Rutgers University, Piscataway, NJ 08854, USA

Abstract In this paper, we analyze several experiments that address the effects of electron-electron interactions in 2D electron (hole) systems in the regime of low carrier density. The interaction effects result in renormalization of the effective spin susceptibility, effective mass, and g^*-factor. We found a good agreement among the data obtained for different 2D electron systems by several experimental teams using different measuring techniques. We conclude that the renormalization is not strongly affected by the material or sample-dependent parameters such as the potential well width, disorder (the carrier mobility), and the bare (band) mass. We demonstrated that the apparent disagreement between the reported results on various 2D electron systems originates mainly from different interpretations of similar "raw" data. Several important issues should be taken into account in the data processing, among them the dependences of the effective mass and spin susceptibility on the in-plane field, and the temperature dependence of the Dingle temperature. The remaining disagreement between the data for various 2D electron systems, on one hand, and the 2D hole system in GaAs, on the other hand, may indicate more complex character of electron-electron interactions in the latter system.

Keywords: low-dimensional electron systems, electron-electron interactions, Fermi-liquid effects

1. Introduction

Understanding the properties of strongly interacting and disordered two-dimensional (2D) electron systems represents an outstanding problem of mod-

ern condensed matter physics. The apparent "2D metal-insulator transition" (2D MIT) is one of the puzzling phenomena that are still waiting for an adequate theoretical description [1, 2]. Figure 1 shows that the transition from the "metallic" to "insulating" behavior occurs as the density of electrons n is decreased below a certain critical value n_c. The strength of electron-electron ($e-e$) interactions is characterized by the ratio of the Coulomb interaction energy to the Fermi energy. This ratio, r_s, increases $\propto 1/n^{1/2}$ [3] and reaches ~ 10 at $n \approx n_c$; this suggests that the $e-e$ interactions might be one of the major driving forces in the phenomenon. Thus, better understanding of the properties of 2D systems at low densities, and, in particular, in the critical regime [4] in the vicinity of the apparent 2D MIT, requires quantitative characterization of electron-electron interactions.

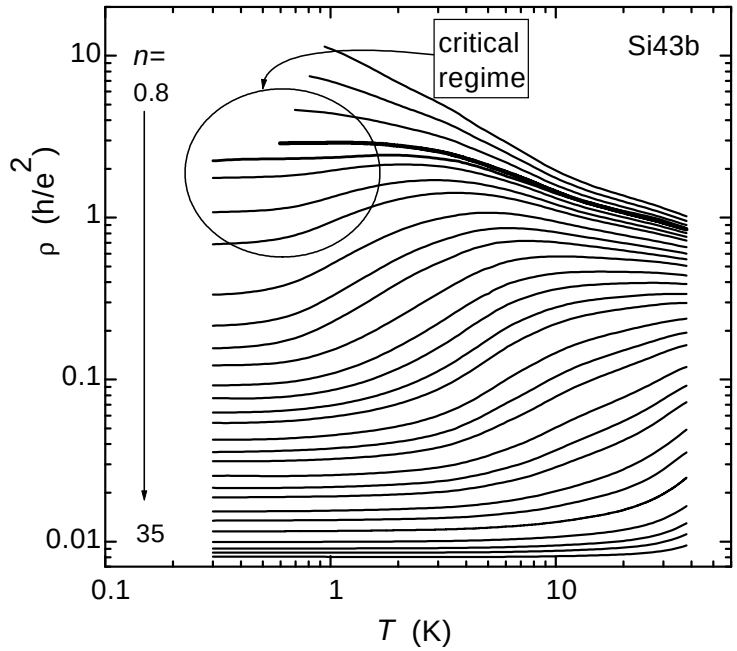

Figure 19.1. Temperature dependences of the resistivity for Si-MOS device over a wide density range, 0.8 to $35 \times 10^{11}\text{cm}^{-2}$.

Within the framework of Fermi-liquid theory, the interactions lead to renormalization of the effective quasiparticle parameters, such as the spin susceptibility χ^*, effective mass m^*, Landé factor g^*, and compressibility κ^*. Measurements of these renormalized parameters are the main source of experimental information on interactions. The renormalizations are described by harmon-

ics of the Fermi-liquid interaction in the singlet (symmetric, (s)) and triplet (antisymmetric, (a)) channels, the first of them being:

$$F_0^a = \frac{2}{g^*} - 1, \qquad F_1^s = 2\left(\frac{m^*}{m_b} - 1\right). \tag{19.1}$$

Here g_b and m_b are the band values of the g-factor and mass, respectively.

Recently, as a result of extensive experimental efforts, rich information on the renormalized quasiparticle parameters has become available for 2D systems. The corresponding results were obtained by different techniques and for different material systems. At first sight, the data sets in different publications seem to differ from each other a great deal. Our goal is to review briefly the available data and to analyze the sources of their diversity. We find that, in fact, the apparent diversity between various results originates mainly from different interpretation of *similar* "raw" data. Being treated on the same footing, most experimental data do agree with each other. The remaining disagreement between the data for p-type GaAs, on one hand, and the other systems, on the other hand, may indicate more complex character of interactions in the former 2D hole system.

2. Renormalized spin susceptibility

Several experimental techniques have been used for measuring the renormalized spin susceptibility χ^*, such as
(i) analysis of the beating pattern of Shubnikov-de Haas (SdH) oscillations in weak tilted or crossed magnetic fields [5–8];
(ii) fitting the temperature- and magnetic field dependences of the resistivity [9–12] with the quantum corrections theory [13, 14];
(iii) the magnetoresistance scaling in strong fields [15–17];
(iv) measuring the "saturation" or hump in magnetoresistance in strong in-plane fields [17–22];
(v) measuring the thermodynamic magnetization [23].
We compare below the available experimental results.

(1) SdH oscillations: n-Si and n-GaAs.
Figure 19.2 shows the $\chi^*(r_s)$ data obtained by Okamoto et al. [5] for n-(100)Si-MOS system by observing how the first harmonic of SdH oscillations vanishes in tilted magnetic fields (the so called "spin-zero" condition, which corresponds to the equality $g^*\mu_B B_{\rm tot} = \hbar\omega_c/2$, where $B_{\rm tot} = \sqrt{B_\perp^2 + B_\parallel^2}$ and μ_B is the Bohr magneton). More recent results [6] on n-(100)SiMOS samples have been obtained from the SdH interference pattern in weak crossed magnetic fields [7]; they extend the earlier data to both higher and lower r_s values. It is worth noting that the data presented in Fig. 19.2 have been obtained for many Si-MOS samples fabricated by different manufacturers [6, 5]; the peak mobilities

for these samples range by a factor of ~ 2. Nevertheless, there is a good agreement between the data for different samples. We conclude therefore that *the effect of disorder on the renormalization of χ^* at $n > n_c$ is negligible or, at least, weak.*

As seen from Fig. 19.2, the data on n-channel Si-MOS samples are in a reasonable agreement with the data obtained by Zhu et al. [8] for n-type GaAs/AlGaAs samples using a similar technique (measuring SdH effect in tilted magnetic fields). Because of a smaller (by a factor of 3) electron effective mass in GaAs, similar r_s values have been realized for the electron density 10 times lower than in Si-MOS samples. The width of the confining potential well in such GaAs/AlGaAs heterojunctions is greater by a factor of 6 than in (100) Si-MOS, due to a smaller mass m_z, lower electron density, and higher dielectric constant. This significant difference in the thickness of 2D layers may be one of the reasons for the 20% difference between the χ^*-data in n-GaAs and n-SiMOS samples seen in Fig. 19.2; at the same time, the minor difference indicates that *the effect of the width of the potential well on renormalization of χ^* is not strong*; recently, this effect has been studied in Ref. [20].

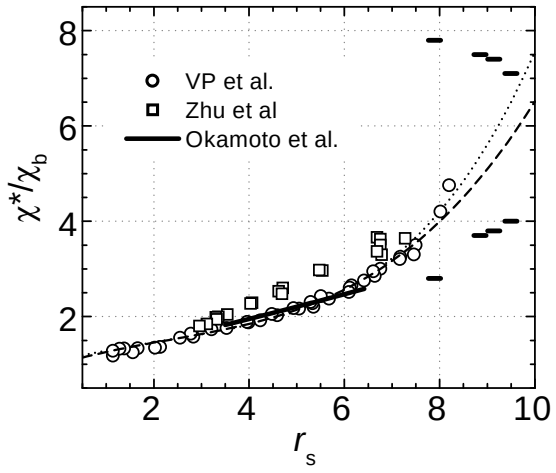

Figure 19.2. Renormalized spin susceptibility measured by SdH effect in tilted or crossed fields on n-SiMOS by Okamoto et al. [5], Pudalov et al [6], and on n-GaAs/AlGaAs by Zhu et al. [8]. Horizontal bars depict the upper and lower limits on the χ^* values, determined from the sign of SdH oscillations, measured at $T = 0.027$mK for sample Si5 [24]. Dashed and dotted lines show two examples of interpolation of the data [5, 6].

The SdH experiments provide the direct measurement of χ^* in weak perpendicular and in-plane magnetic fields $\hbar\omega_c \ll E_F$, $g^*\mu_B B_{\rm tot} \ll E_F$ [6, 7]. Under such conditions, the quantum oscillations of the Fermi energy may be ne-

glected, and the magnetization remains a linear function of B, $\chi^*(B_{\rm tot}) \approx \chi_0^*$. Also, under such experimental conditions, the filling factor is large, $\nu = (nh)/(eB_\perp) \gg 1$ and the amplitude of oscillations is small $|\delta\rho_{xx}|/\rho_{xx} \ll 1$. Figure 19.3 shows, on the $\rho - B_\perp$ plane, the domain of the weak magnetic fields, $\nu > 6$, where the SdH oscillations have been measured in Refs. [6, 24]. As the perpendicular magnetic field increases further (and ν decreases), the SdH oscillations at high density $n \gg n_c$ transform into the quantum Hall effect; for low densities, $n \approx n_c$, the SdH oscillations transform into the so called "reentrant QHE-insulator"(QHE-I) transitions [25, 26]. The uppermost curve (open circles) presents the $\rho(B)$ variations in the regime of QHE-I transitions [25, 26]), measured for a density slightly larger (by 4%) than the critical value n_c. This diagram is only qualitative, because the n_c value is sample-dependent.

Regime of low densities. In the vicinity of the critical density $n \approx n_c$, the number of observed oscillations decreases, their period increases, and the interpretation of the interference pattern becomes more difficult, thus limiting the range of direct measurements of $\chi^*(r_s)$.

The horizontal bars in Fig. 19.2 are obtained from consideration of the sign and period of SdH oscillations [24] as explained below. They show the upper limit for χ^*, calculated from the data reported in Refs. [6, 26, 24]. Figure 19.3 b demonstrates that in the density range $0.7 < n < 1 \times 10^{11}\text{cm}^{-2}$, the oscillatory ρ_{xx} (beyond the magnetic field enhanced $\nu = 1$ valley gap) has minima at filling factors

$$\nu = (4i - 2), \qquad i = 1, 2, 3..., \tag{19.2}$$

rather than at $\nu = 4i$ (in (100) Si-MOSFETs, the valley degeneracy $g_v = 2$). The latter situation is typical for high densities and corresponds to inequality $g^*\mu_B B < \hbar\omega_c^*/2$.

In other words, the sign of oscillations at low densities is reversed. This fact is fully consistent with other observations (see, e.g., Fig. 2 of Ref. [24], Fig. 1 of Ref. [27], and Figs. 1-3 of Ref. [28]). As figure 19.2 shows, the ratio χ^*/χ_b exceeds $1/2m_b = 2.6$ at $r_s \approx 6$; the first harmonic of oscillations disappears at this density (so called "spin-zero"), and the oscillations change sign for lower densities. Since the sign of the SdH oscillations is determined by the ratio of the Zeeman to cyclotron splitting [29, 30]

$$\cos\left(\pi\frac{g^*\mu_B B}{\hbar\omega_c^*}\right) \equiv \cos\left(\pi\frac{\chi^*}{\chi_b}m_b\right), \tag{19.3}$$

it was concluded in Ref. [24] that, in order to have negative sign in the range $10 > r_s > 6$, the spin susceptibility χ^* must obey the following inequality:

$$2.6 = \frac{1}{2m_b} < \frac{\chi^*}{\chi_b} < \frac{3}{2m_b} = 7.9. \tag{19.4}$$

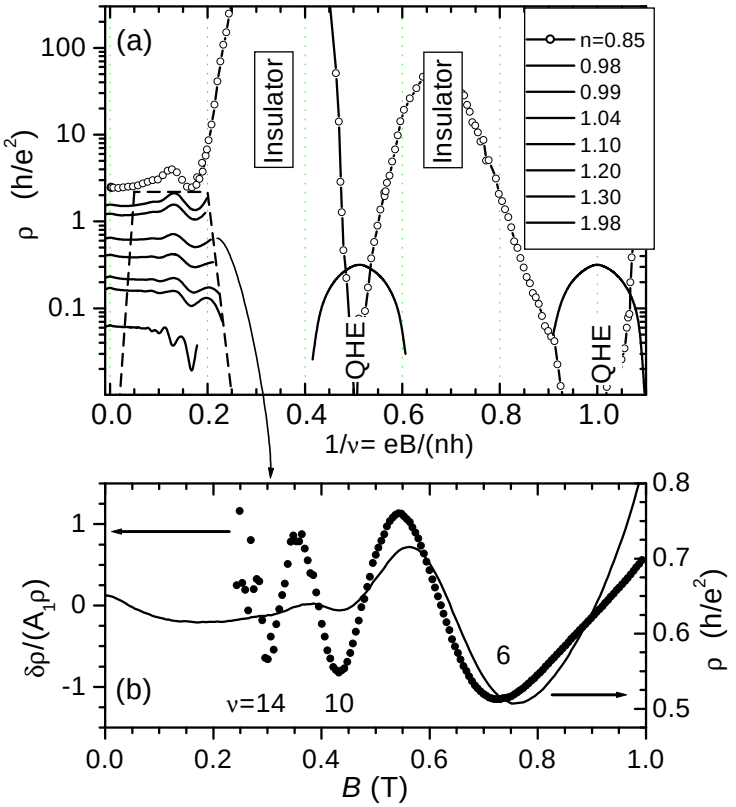

Figure 19.3. (a) Overall view of the SdH oscillations in low fields at different densities. Empty circles show the ρ_{xx} oscillations for sample Si9 in high fields, corresponding to the reentrant QHE-insulator transitions [26]. (b) Expanded view of one of the $\rho_{xx}(B)$ curves ($n = 1.04 \times 10^{11}\text{cm}^{-2}$ (right axis) and its oscillatory component normalized by the amplitude of the first harmonic $A_1(B)$ (left axis) [6]. Dashed line confines the region of the SdH measurements in Refs. [6, 24].

Thus, Eq. (19.2) and Eq. (19.4) enable us to set the upper and lower limits for χ^* [24], which are shown by horizontal bars in Fig. 19.2 at $r_s = 7.9 - 9.5$. As density decreases (and r_s increases), due to finite perpendicular fields, in which the SdH oscillations were measured, the condition Eq. (19.4) becomes a bit more restrictive, which leads to narrowing the interval between the upper and lower bars [24].

(2) Magnetoresistance in the in-plane field.

Monotonic magnetoresistance (MR) in the in-plane field exhibits a well-defined saturation for the n-type Si MOSFETs [31–36, 15] or a hump for the n- or p-

type 2D GaAs systems [18, 21, 19, 20, 9, 8]. With increasing mobility (and corresponding decreasing critical n_c density), the latter hump becomes more pronounced; it resembles the sharp transition to the $R(B_\parallel)$ saturation in Si-MOS [37].

The hump or saturation of the in-plane magnetoresistance have been interpreted in Refs. [19, 17] as a signature of complete spin polarization $B_{\rm pol}$. This treatment is also supported by the experiments by Vitkalov et al. [36, 38], who found that the frequency doubling of SdH oscillations coincides with the onset of saturation of the in-plane magnetoresistance. Another approach to the high field measurements of χ^* is based on the scaling of $R(B_\parallel)$ data [16, 15]: by scaling, the $R(B_\parallel)$ data for different densities are forced to collapse onto each other. This procedure is essentially the high-field one, $g^*\mu B \sim 0.6E_F$, as the chosen scaling field $B_{\rm sc} \approx 0.3B_{\rm pol}$.

The features in $\rho(B_\parallel)$ are observed at a field $B_{\rm sat}$, which is close to the estimated field of the complete spin polarization [34]:

$$B_{\rm sat} \approx B_{\rm pol} = 2E_F/g^*\mu_B. \tag{19.5}$$

By assuming that $B_{\rm pol} = B_{\rm sat}$ and using the standard expression for the 2D density of states, ${\rm DOS} = m^* g_v/\pi\hbar^2$, one can estimate χ^* from measurements of the characteristic field $B_{\rm sat}$:

$$g^* m^* = \frac{2n\pi\hbar^2}{B_{\rm sat} g_v \mu_B}. \tag{19.6}$$

Evaluation of χ^* from the aforementioned experiments in strong fields and from Eqs. (19.6) and (19.5) is based on the following assumptions: (i) $\chi^* \propto g^*m^*$ is $B_\parallel$-independent; (ii) m^* and 2D DOS are energy-independent. In general, both assumptions are dubious. Nevertheless, for some samples, Eqs. (19.6) and (19.5) may give plausible results over a limited range of densities. For example, the low-field SdH data and the high field magnetoresistance data were found to differ only by $\leq 12\%$ over the density range $(1-10)\times 10^{11}{\rm cm}^{-2}$. More detailed critical analysis of the in-plane MR data may be found in Refs. [20, 22, 23, 39, 40, 8].

An interesting interpretation of the MR data has been suggested in Ref. [16], where the $1/\chi^*(n)$ dependence determined down to $n = 1.08\times 10^{11}{\rm cm}^{-2}$, was linearly extrapolated to zero at $n \approx 0.85\times 10^{11}{\rm cm}^{-2}$ and interpreted as an indication of the ferromagnetic instability at this density. Our data, obtained from the analysis of the period and sign of SdH oscillations at lower densities [24], do not support this interpretation:

(i) in the whole domain of densities and fields depicted in Fig. 19.3, no doubling of the frequency of SdH oscillations is observed, which proves that the 2D system remains spin-unpolarized (see e.g., Fig. 19.3;

(ii) the sign of the SdH oscillations [see Eq. (19.2) and the discussion above]

enables us to estimate the upper limit on χ^* (see bars in Fig. 19.2) in the interval of $r_s = 8-9.5$, i.e. $n = (1.08-0.77)\times 10^{11}\text{cm}^{-2}$. Note that the latter interval includes critical n_c values for most of the high mobility Si-MOS samples, in particular, those used in Ref. [16].

(3) Temperature dependence of χ^*.

In order to test whether or not the enhanced spin susceptibility χ^* depend strongly on temperature, we measured the interference pattern of SdH oscillations for various temperatures (see Fig. 19.4) and for different densities, and thus determined the temperature dependence of χ^*. The results shown in Fig. 19.4 reveal only weak temperature variations of $\chi^*(T)$, within 2% in the studied T range. We therefore can safely neglect the effect of temperature in comparison of different sets of data.

There are several possible reasons for the disagreement between the high-field and low-field data; they are considered below.

(4) Effect of disorder on the high-field MR data.

Firstly, it has been shown in Refs. [22, 39] that the saturation field $B_{\rm sat}$ and the high-field MR for Si-MOSFETs [40] are strongly sample- (disorder-) dependent. In particular, for a given density (and, hence, given E_F), $B_{\rm sat}$ can vary by as much as a factor of two for the samples with different mobilities. It was suggested in Refs. [22, 41, 17] that these variations are caused by the localized states, so that Eq. (19.6) might be thought to hold only for a "disorder-free" sample [17]. However, by extrapolating the measured $B_{\rm sat}$ fields [22, 39] for samples with different peak mobilities to $1/\mu^{\rm peak} \to 0$, one obtains a "disorder free" $B_{\rm sat}^{\mu=\infty}$ value, which overshoots the spin polarizing field [39], i.e. $B_{\rm sat}^{\mu=\infty} > B_{\rm pol}$. This suggests that the structure of the localized states below the Fermi level is non-trivial [42]. Since $B_{\rm sat}$ crosses $B_{\rm pol}$, the two quantities become equal at some mobility value. For this nontrivial reason, the estimate Eq. (19.6) provides correct results [43] for some samples with intermediate mobilities; nevertheless, for lower densities $n \approx n_c$, deviations from the SdH data are observed, as discussed in Ref. [44].

(5) Magnetic field dependence of χ^*.

Secondly, both parameters m^* and g^* (and $\chi^* \propto g^* m^*$) that enter Eqs. (19.5), (19.6) depend on the in-plane field. The $m^*(B_\parallel)$ dependence is mainly an orbital effect [45]; it is very strong for n-GaAs samples with wider potential well [8, 20]. In contrast, the $g^*(B_\parallel)$ dependence is apparently a spin-related effect [8, 46]. The dependence of m^* and g^* on $B_\parallel$ is another reason for the deviation of the high-field χ^* values from the low field results of SdH measurements. In GaAs, the difference between the low-$B_\parallel$ and high-$B_\parallel$ data is dramatic [8, 20]: the density dependence of χ^* derived for 2D electrons in GaAs on the basis of the $R(B_\parallel)$ measurements in high fields is non-monotonic, whereas the same samples demonstrated a monotonic $\chi^*(n)$ dependence in low fields (see Fig. 19.2) [8, 20]. It is plausible, therefore, that ignoring the $m^*(B_\parallel)$ orbital

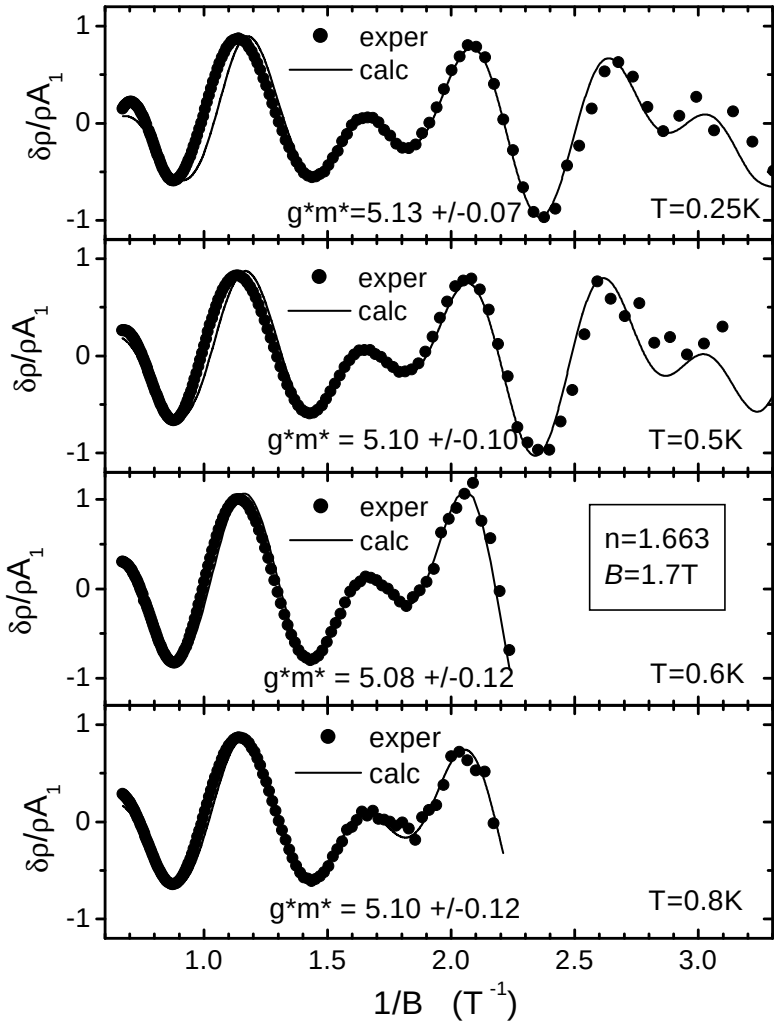

Figure 19.4. Typical evolution of the interference pattern in SdH oscillations with temperature. The oscillations are normalized by the amplitude of the first harmonic [6].

dependence causes the non-monotonic density dependence of F_0^a, obtained in Ref. [37] for 2D holes in GaAs in the dilute regime $p \sim 10^{10}\text{cm}^{-2}$, in which the potential well is very wide. The $m^*(B_\parallel)$ dependence is also present in Si-MOS samples [46], though it is weaker than in GaAs owing to a narrower potential well; as the density decreases and potential well gets wider, this orbital effect should have a stronger influence on the results of high-field MR measurements.

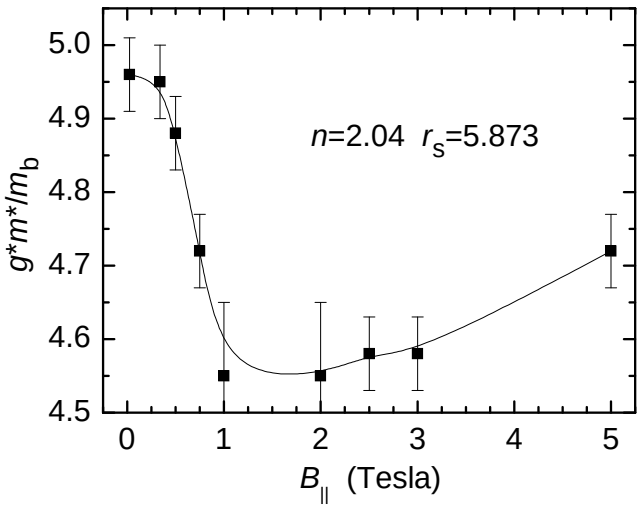

Figure 19.5. Typical dependence of the spin susceptibility on the in-plane magnetic field, measured for n-Si-MOS sample at $T \approx 0.15$K. Density is given in units of 10^{11}cm^{-2}.

(6) Magnetization measurements.

Another important source of experimental information on the spin susceptibility are the thermodynamic magnetization measurements, performed recently by Reznikov et al. [23] on Si-MOS samples. Over the density range $(3-9)\times 10^{11}\text{cm}^{-2}$, the measured dM/dB is in agreement with the SdH data on χ^*. The contribution of the localized states to the measured magnetization impedes the detailed quantitative comparison with the SdH data at lower densities. Nevertheless, two important results at low densities are in a good agreement with the SdH data: (i) the spin susceptibility remains finite down to the lowest density (thus confirming the absence of the spontaneous magnetization transition), and (ii) the magnetization is nonlinear in $B_\parallel$ field with χ^* varying with field qualitatively similar to that shown in Fig. 19.5.

3. Effective mass and g-factor

Historically, experimental data on the effective mass in 2D systems have always been controversial (for a review of the earlier data, see [3]). The data on m^* have been obtained mainly from the temperature dependence of SdH oscillations. Even within the same approach, the data from different experiments disagreed with each other at low densities. With the advent of high mobility samples, much lower densities became accessible. However, the general trend remained the same: disagreement between different sets of data grew

as the density was decreased; this disagreement becomes noticeable when $k_F l$ becomes smaller than ~ 5.

Figure 19.6 shows that the data for Si-MOS samples determined in Refs. [6, 47, 48] are close to each other only at $n > 2.5 \cdot 10^{11}$ cm^{-2} ($r_s < 5$). At lower densities, at first sight, there is a factor of ~ 1.5 disagreement between the data of Refs. [6] and [48] (closed and open symbols, respectively), which is discouraging. However, we show below that the apparent disagreement stems from different interpretations of raw data. When treated on the same footing, the data agree reasonably well with each other down to the lowest explored density $n \approx 1 \times 10^{11}$ cm^{-2} (i.e. $r_s \approx 8$).

One might suspect that the difference in the extracted m^* values is due to the different temperature ranges in different experiments ($T = 0.15 - 1$ K and $0.3 - 3$ K in Ref. [6] and $T = 0.05 - 0.25$ K in Ref. [48]). However, the data in Fig. 19.4 do not reveal a strong T-dependence of χ^*. Since χ^* is proportional to $g^* m^*$, one has to assume that the temperature dependences of m^* and g^* must compensate each other; such compensation is highly unlikely.

In order to determine the effective mass from the temperature dependence of the amplitude of SdH oscillations, one needs a model; below we consider the models which are used in calculations of m^*. The open squares [48] and open circles [6] in Fig. 19.6 are obtained by using the same model of non-interacting Fermi gas, for which the amplitude of SdH oscillations is given by the Lifshitz-Kosevich (LK) formula [29]. The effective mass in this model is derived from the T-dependence of the amplitude, which in the limit of $kT \gg \hbar\omega_c$ can be expressed as:

$$-\frac{e\hbar H}{2\pi^2 k_B c} \ln |\delta\rho_{xx}/\rho_{xx}| \approx m^*(T + T_D). \tag{19.7}$$

If one assumes that the Dingle temperature T_D is *temperature independent*, the calculated mass appears to depend on the temperature interval of measurements [6]: the higher the temperature, the larger the mass. Note that the direct measurements of $g^* m^*(T)$ do not reveal any substantial T-dependence of this quantity. Moreover, the mass value calculated in this way was found to be somewhat different for samples with different mobilities (i.e. τ values).

We believe that the aforementioned inconsistencies are caused by assuming that T_D is *temperature independent*. This assumption is not justified, even if the resistance is temperature-independent over the studied T range (see, e.g. [49]). However, in a typical experimental situation, determination of m^* requires measurements of the oscillation amplitude over a wide temperature range, where ρ is strongly T-dependent [12] owing to the interaction corrections [13].

In Ref. [6], in order to determine m^* in a strongly-interacting 2D electron system in Si MOSFETs, another approach has been suggested, in which $T_D(T)$

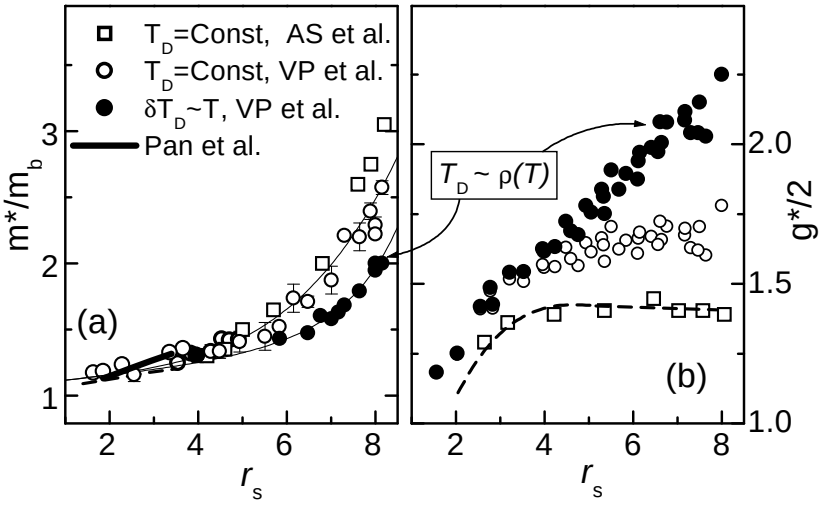

Figure 19.6. Renormalized effective mass of electrons m^* (a) and renormalized g-factor (b) determined with Si-MOS samples in different experiments as denoted in the legend. Data shown by open boxes and circles are from Refs. [48], and [6], correspondingly, calculated using the LK formula Eq. (19.7). Closed circles are the data from Ref. [6] obtained using Eq. (19.8).

was assumed to reflect the temperature dependence of the resistivity $\varrho = \varrho_0 + \beta(n)T\tau$:

$$T_D^*(T) \approx T_D(1 + \beta(n)T\tau). \tag{19.8}$$

This empirical approach eliminates largely the disagreement between the results on m^* for the same sample, obtained in different temperature intervals, and between the results obtained for different samples. This conjecture has been supported recently by the theoretical study [49]. The data shown in Fig. 19.6 by closed circles are obtained within this approach [6]; we believe, they represent more reliable m^* data, which are consistent with the other types of measurements (e.g., with the analysis [12] of $\rho(T)$ in terms of the theory of interaction corrections in the ballistic regime).

We will verify now whether or not the approach of Eq. (19.8) leads to convergence of the results from Ref. [48] (open boxes) and Ref. [6] (closed points). In order to do this, we use the $\sigma(T)$ dependences reported in Ref. [10] for the same samples. We show below how the results on m^* from Ref. [48] could be "corrected" in order to take into account a finite $d\sigma/dT$). The open-box data point with the highest r_s value in Fig. 19.6 corresponds to the density $n = 1.03 \times 10^{11}\text{cm}^{-2}$. The $\sigma(T)$ curves are reported in Fig. 1 of Ref. [10]

for two nearest density values, $n = 1.01$ and 1.08×10^{11}cm^{-2}. For simplicity, over the range of the SdH measurements $T = 0.05 - 0.25$K [48], the $\sigma(T)$ dependence may be approximated by a linear T-dependence with the slope $d\ln\sigma/dT \approx -1/$K. According to Eq. (19.8), we now use the $\sigma(T)$ slope together with $T_D \approx 0.2$K for the range $T = 0.05 - 0.25$ K as reported in Ref. [48]. As a result, we obtain $T_D = T_{D0}(1+T)$ and, to the first approximation, $m^*0.833[T + T_{D0}(1+T)] = m^*0.833[1.2T + 0.24]$ for the temperature dependence of the logarithm of the oscillation amplitude. The exact procedure of the non-linear data fitting based on Eq. (19.8) requires more thorough consideration; we describe here a simplified step-by step procedure of fitting. At the 2nd step one obtains $0.8m^*[T1.24 + 0.248]$, etc. All the above functions fit equally well the same raw data (i.e. the T-dependence of the amplitude of oscillations), but with different masses. Finally, the procedure converges with the mass that is by $\sim 20\%$ smaller and the Dingle temperature that is by 25% larger than the initial values, respectively. As a result, the disagreement between the data at this n in Fig. 19.6 is reduced from 50% to about 25%.

We have repeated the same procedure at every density, for which the $\sigma(T)$ curve is known for samples used in Ref. [48]. For the lower densities, similarity between the results of Refs. [6] and [48] is even more striking. For example, for the second data point ($n = 1.08 \times 10^{11}$cm^{-2}, $r_s = 7.9$), the initial disagreement between the masses is 43%: $m^*/m_b = 2.75$ (open boxes) versus 1.92 (closed dots). After applying the same procedure of the non-linear fitting with $d\ln\sigma/dT = -0.72$K, and initial $T_D = 0.25$K, we obtain the corrected values $T_{D0} = 0.333$K and $m^*/m_b = 2.06$; the latter value differs only by 7% from our data (closed circles). At the highest density, $n = 2.4 \times 10^{11}$cm^{-2} ($r_s = 5.37$, for which the $\sigma(T)$ dependences are shown in Fig. 1 of Ref. [10], the mass correction is also $\sim 6\%$.

Reduction of the m^* values from Ref. [48] (by taking into account the T-dependence of T_D) leads to re-evaluation of g^*: since $\chi^*(n)$ is known with higher accuracy, the decrease in m^* leads to the corresponding increase in $g^* \propto \chi^*/m^*$. The $g^*(r_s)$ dependence becomes monotonic, and comes into agreement with the earlier data shown in Fig. 19.6,b as closed dots.

3.1 F_0^a values

The F_0^a values are determined from the renormalized g^* factor. Firstly, as expected, we find that all $g^*(r_s)$ data for (100) n-Si [6] and vicinal to (100) Si-MOS samples [50] are rather close to each other. Secondly, after the aforementioned correction has been made to m^*, the data from Ref. [48] become consistent with the data from Ref. [6]. Note that the $m^*(r_s)$ and F_0^a data for n-GaAs samples, determined on the basis of approach Eq. (19.8), are currently

unavailable. We focus below on comparison with p-GaAs, for which the disagreement is dramatic, as Fig. 19.7 shows.

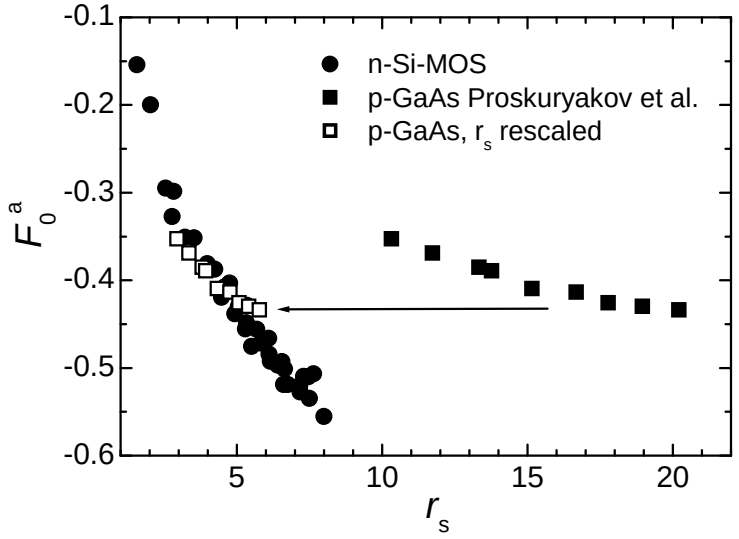

Figure 19.7. Comparison of the F_0^a values determined for n-SiMOS [6] and for p-GaAs/AlGaAs [9]; the latter data are also shown versus r_s without and with scaling down by a factor of 3.5.

Comparison with p-GaAs.

With increasing quality of p-GaAs/AlGaAs samples, the critical values of r_s that corresponds to the apparent 2D metal-insulator crossover grew from 17 [9] to 37 [37], and finally to 57 [51]. Observation of a non-insulating behavior at such unprecedently high r_s values represents a puzzle by itself; two other puzzles are the observed non-monotonic behavior of the renormalized g-factor (and F_0^a) with r_s [37] and r_s-independent m^* [9]. Even if the nonmonotonic $g^*(r_s)$ dependence might be explained by the orbital effects (i.e. the $m^*(B_\parallel)$ dependence) [8], the difference between 2D holes in GaAs and other 2D systems remains dramatic.

Clearly, the dependences $m^*(r_s)$ and $g^*(r_s)$ for p-GaAs cannot be obtained by extrapolating the Si MOS data to higher r_s values (see Fig. 19.6). Not surprisingly, therefore, that the F_0^a data, deduced in Refs. [9, 52] from the temperature dependence of the conductivity, differ substantially from the values determined for n-Si- and n-GaAs-based structures (see Fig. 19.7). It is highly unlikely that the values of $F_0^a(r_s)$ "jump up" around $r_s \sim 10$ (where the data are currently missing); such possibility is also at odds with the numerical results. Rather, this non-monotonic dependence might signal either the lack of the

universal dependence $F_0^a(r_s)$ or an incorrect quantification of the effective interaction strength in different systems.

To choose between the aforementioned options, let us compare the charge transport in n-type and p-GaAs systems in the low-density regime. It is well-known that the experimental data for various 2D electron and hole systems studied so far exhibit a number of empirical similarities (quantitative within the same host material and qualitative - for different systems). The two of them are: (i) the relationship between the "critical" ρ_c and r_s values, and (ii) the magnitude of the resistivity drop $\Delta\rho(T)/\rho_D$ at a given resistivity ρ_D value. Both dependences imply a similar mechanism: the higher the quality of the sample, the larger the critical r_s (i.e. the lower n_c), F_0^a, ρ_c and the magnitude of the resistance drop. These qualitative features have been explained by the theory [13], where the only sample- (or disorder-) dependent parameter is the mean free time τ (the higher τ, the stronger the "metallic" $\rho(T)$ dependence).

The low density p-GaAs [9, 37, 51] samples demonstrate different features: on the one hand, the r_s-values are extremely high (thus indicating a high sample quality and strong interactions), on the other hand, the signatures of the metallic behaviour are rather weak. For the highest r_s data [37, 51] the renormalized Fermi energy is so small (~ 0.1K) that the 2D systems becomes non-degenerate very quickly as T grows. This might explain the weak magnitude of the resistance drop in the measurements of Ref. [37, 51]. However, this line of reasoning is irrelevant to the higher-density (311) p-GaAs samples [9], in which the Fermi energy is larger. In order to bring the above data for p-GaAs into agreement with other data, one has to scale the r_s values down by a factor of 6 [9] and factor of 8 [37].

It might be, therefore, that the effective $e-e$ interactions are weaker in p-GaAs samples than in the other systems for the same r_s value, owing to a more complicated physics of the multivalley band structure and strong spin-orbit effects. If this is the case, the interactions in p-GaAs samples cannot be adequately quantified with a single parameter r_s. We illustrate this in Fig. 19.7 by a simple rescaling of the effective r_s values for the data on p-GaAs [9]. Despite the raw data differ substantially, they come into a reasonable agreement when r_s for p-GaAs is scaled down by an empirical factor 3.5. Of course, from this rescaling, it is impossible to conclude whether the effective r_s values should be increased for n-Si- and n-GaAs- based structures, or decreased for p-GaAs; however, the multitude of the material systems which show reasonably consistent data, points at a somewhat more complex behavior in p-GaAs. The same empirical scaling procedure applied to the $m^*(r_s)$ data for p-GaAs helps to resolve another puzzle. The data for the effective mass that were found in Ref. [9] to be r_s independent over the range $r_s = 10-17$, after such rescaling will fall into the range $r_s = 2.8-4.8$, where the mass variations with r_s are small (see Fig. 19.6).

4. Summary

To summarize, we compared various experimental data on the renormalization of the effective spin susceptibility, effective mass, and g^*-factor. If the data are considered on the same footing, one finds a good agreement between different sets of data, measured by different experimental teams using different experimental techniques, and for different 2D electron systems. The consistency of the data provides one more evidence that the renormalization is indeed caused by the Fermi-liquid effects. The renormalization is not strongly affected by material- and sample-dependent parameters such as the width of the potential well, disorder (sample mobility) and the band mass value. The apparent disagreement between the reported results is caused mainly by different interpretation of similar raw data. Among the most important issues to be taken into account in the data processing, there are the dependences of the effective mass and spin susceptibility on the in-plane field, and the temperature dependence of the "Dingle temperature" (the latter is intrinsic for strongly-interacting systems). The remaining disagreement with the data for 2D hole system in GaAs suggests that the character of the effective electron-electron interaction is more complex in this system; this important issue deserves thorough theoretical attention.

Acknowledgments

The work was supported in part by NSF, ARO MURI, INTAS, RFBR, and the Russian grants from the Ministry for Science and Technology, Programs of the RAS, and the Presidential Program of the support of leading scientific schools.

References

[1] S. V. Kravchenko, G. V. Kravchenko, J. E. Furneaux, V. M. Pudalov, and M. D'Iorio, Phys. Rev. B **50**, 8039 (1994).

[2] S. V. Kravchenko, G. E. Bowler, J. E. Furneaux, V. M. Pudalov, and M. D'Iorio, Phys. Rev. B **51**, 7038 (1995).

[3] T. Ando, A. B. Fowler, F. Stern, Rev. Mod. Phys. **54**, 432 (1982).

[4] B. L. Altshuler, D. L. Maslov, and V.M. Pudalov, Physica E, **9**, 2092001.

[5] T. Okamoto, K. Hosoya, S. Kawaji, and A. Yagi, Phys. Rev. Lett. **82**, 3875 (1999).

[6] V. M. Pudalov, M. E. Gershenson, H. Kojima, N. Butch, E. M. Dizhur, G. Brunthaler, A. Prinz, and G. Bauer, Phys. Rev. Lett. **88**, 196404 (2002).

[7] M. E. Gershenson, V. M. Pudalov, H. Kojima, E. M. Dizhur, G. Brunthaler, A. Prinz, and G. Bauer, Physica E, **12**, 585 (2002).

[8] J. Zhu, H. L. Stormer, L. N. Pfeiffer, K. W. Baldwin, and K. W. West, Phys. Rev. Lett. **90**, 056805 (2003).

[9] Y. Y. Proskuryakov, A. K. Savchenko, S. S. Safonov, M. Pepper, M. Y. Simons, and D. A. Ritchie, Phys. Rev. Lett. **89**, 076406 (2002).

[10] A. A. Shashkin, S. V. Kravchenko, V. T. Dolgopolov, and T. M. Klapwijk, Phys. Rev. B **66**, 076303 (2002).

[11] S. A. Vitkalov, K. James, B. N. Narozhny, M. P. Sarachik, and T. M. Klapwijk, Phys. Rev. B **67**, 113310 (2003).

[12] V. M. Pudalov, M. E. Gershenson, H. Kojima, G. Brunthaler, A. Prinz, and G. Bauer, Phys. Rev. Lett. **91**, 126403 (2003).

[13] G. Zala, B. N. Narozhny, and I. L. Aleiner., Phys. Rev. B **64**,214204 (2001); Phys. Rev. B **65**, 020201 (2001).

[14] I. V. Gornyi, and A. D. Mirlin, cond-mat/306029.

[15] S. A. Vitkalov, H. Zheng, K. M. Mertes, M. P. Sarachik, and T. M. Klapwijk, Phys. Rev. Lett. **87**, 086401 (2001).

[16] A. A. Shashkin, S. V. Kravchenko, V. T. Dolgopolov, and T. M. Klapwijk, Phys. Rev. Lett. **87**, 086801 (2001).

[17] S. A. Vitkalov, M. P. Sarachik, and T. M. Klapwijk, Phys. Rev. B **65**, 201106 (2002).

[18] J. Yoon, C. C. Li, D. Shahar, D. C. Tsui, and M. Shayegan, Phys. Rev. Lett. **84**, 4421 (2000).

[19] E. Tutuc, E. P. DePoortere, S. J. Papadakis, and M. Shayegan, Phys. Rev. Lett. **86**, 2858 (2001).

[20] E. Tutuc, E. Melinte, E. P. De Poortere, M. Shayegan and R. Winkler, Phys. Rev. B **67**, 241309 (2003).

[21] E. Tutuc, E. Melinte, and M. Shayegan, Phys. Rev. Lett. **88**, 036805 (2002).

[22] V. M. Pudalov, G. Brunthaler, A. Prinz, and G. Bauer, Phys. Rev. Lett. **88**, 076401 (2001).

[23] O. Prus, Y. Yaish, M. Reznikov, U. Sivan, and V. M. Pudalov Phys. Rev. B **67**, 205407 (2003).

[24] V. M. Pudalov, M. Gershenson, H. Kojima, cond-mat/0110160.

[25] M. D'Iorio, V. M. Pudalov, and S. G. Semenchinckii, Phys. Lett. A **150**, 422 (1990).

[26] M. D'Iorio, V. M. Pudalov, and S. G. Semenchinsky Phys. Rev. B **46**, 15992 (1992).

[27] V. M. Pudalov, M. D'Iorio, J. W. Campbell, JETP Lett., **57**, 608 (1993).

[28] S. V. Kravchenko, A. A. Shashkin, D. A. Bloore, T. M. Klapwijk, Sol. St. Commun. **116**, 495 (2000).

[29] I. M. Lifshitz and A. M. Kosevich, Zh. Eks. Teor. Fiz. **29**, 730 (1955). A. Isihara, L. Smrčka, J. Phys. C: Solid State Phys. **19**, 6777 (1986).

[30] Yu. A. Bychkov, and L. P. Gor'kov, Zh.Exp.Teor. Fiz. **41**, 1592 (1961). [Sov. Phys.: JETP **14**, 1132 (1962)].

[31] D. J. Bishop, R. C. Dynes, D. C. Tsui, Phys. Rev. B **26**, 773 (1982).

[32] D. Simonia, S. V. Kravchenko, M. P. Sarachik, and V. M. Pudalov Phys. Rev. Lett. **79**, 2304 (1997).

[33] V. M. Pudalov, G. Brunthaler, A. Prinz, and G. Bauer, JETP Lett. **65** 932 (1997).

[34] V. M. Pudalov, G. Brunthaler, A. Prinz, and G. Bauer, Physica B **249**, 697 (1998).

[35] K. Eng, X. G. Feng, D. Popović, and S. Washburn, Phys. Rev. Lett. **88**, 136402 (2002).

[36] S. A. Vitkalov, H. Zheng, K. M. Mertes, M. P. Sarachik, and T. M. Klapwijk, Phys. Rev. Lett. **85**, 2164 (2000).

[37] H. Noh, M. P. Lilly, D. C. Tsui, J. A. Simmons, L. N. Pfeiffer, and K. W. West, cond-mat/0206519.

[38] S. A. Vitkalov, M. P. Sarachik, and T. M. Klapwijk, Phys. Rev. B **64**, 073101 (2001).

[39] V. M. Pudalov, G. Brunthaler, A. Prinz, and G. Bauer, cond-mat/0103087.

[40] V. M. Pudalov, M. Gershenson, H. Kojima, cond-mat/0201001.

[41] V. T. Dolgopolov, and A. V. Gold, Phys. Rev. Lett. **89**, 129701 (2002).

[42] V. M. Pudalov, G. Brunthaler, A. Prinz, and G. Bauer, Phys. Rev. Lett. **89**, 129702 (2002).

[43] S. V. Kravchenko, A. Shashkin, V. T. Dolgopolov, Phys. Rev. Lett. **89**, 219701 (2002).

[44] V. M. Pudalov, M. Gershenson, H. Kojima, N. Busch, E. M. Dizhur, G. Brunthaler, A. Prinz, and G. Bauer, Phys. Rev. Lett. **89**, 219702 (2002).

[45] F. Stern, Phys. Rev. Lett. **21**, 1687 (1968).

[46] V. M. Pudalov, M. Gershenson, H. Kojima, to be published elsewhere.

[47] W. Pan, D. C. Tsui, and B. L. Draper, Phys. Rev. B **59**, 10208 (1999).

[48] A. A. Shashkin, M. Rahimi, S. Anissimova, S. V. Kravchenko, V. T. Dolgopolov, and T. M. Klapwijk, Phys. Rev. Lett. **91**, 046403 (2003).

[49] G. W. Martin, D. L. Maslov, M. Reiser, cond-mat/0302054.

[50] Y. Y. Proskuryakov, A. K. Savchenko, S. S. Safonov, M. Pepper, M. Y. Simons, D. A. Ritchie, E. H. Linfield, and Z. D. Kvon, J. Phys. A **36**, 9249 (2003).

[51] H. Noh, M. P. Lilly, D. C. Tsui, J. A. Simmons, L. N. Pfeiffer, and K. W. West, cond-mat/0301301.

[52] L. Li, Y. Y. Proskuryakov, A. K. Savchenko, E. H. Linfield, D. A. Ritchie, Phys. Rev. Lett. **90**, 076802 (2003).